Stable isotopes and hydrogeochemical evolutions of groundwater from a typical seismic fault zone in the Mt. Lushan region, Eastern China

Zhicheng Bao[1], Le Hu[2]*, Jian Xiao[1], Xiaohui Zha[1], Jian Lv[1] and Ying Zhao[1]

[1]Jiangxi Earthquake Angecy, Nanchang, China, [2]Institute of Earthquake Forecasting, China Earthquake Administration, Beijing, China
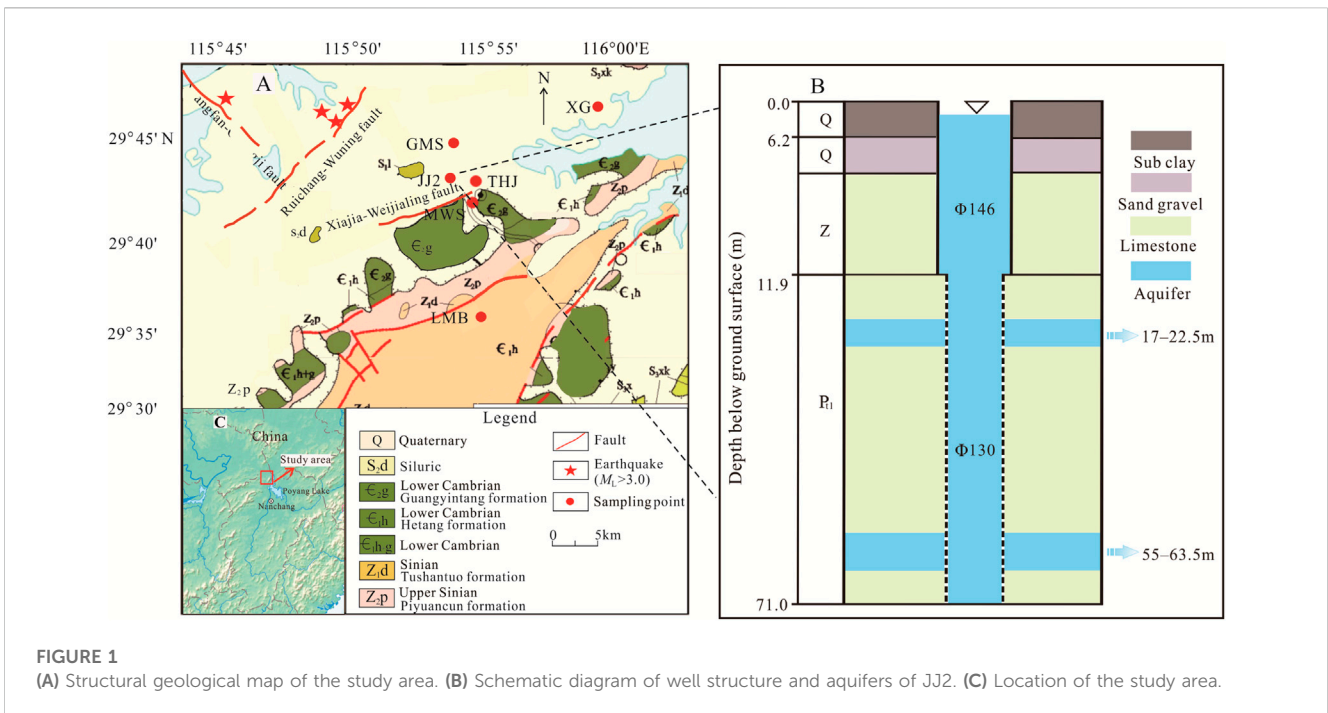
We analyzed the major chemical components, hydrogen (δD) and oxygen isotopes ($\delta^{18}O$), and tritium activity in groundwater from Jiujiang well number 2 (JJ2) as well as atmospheric precipitation and water from the Maweishui spring and Tianhuajing reservoir in the Mt. Lushan region, Eastern China. The results show that the water in JJ2 is of the HCO_3-Ca·Mg type, with ionic components mainly arising from calcite and dolomite mineral dissolution. According to the δD and $\delta^{18}O$ data, the groundwater of JJ2 mainly comes from atmospheric precipitation, and the recharge elevation is 554 m. Results for tritium activity indicate that JJ2 is fed by both an ancient water supply and a new water supply within a period of 10 years. These results demonstrate that JJ2 has characteristics of both shallow and deep circulating water, which implies that aquifers involving two different recharge sources rise to the well surface via different circulation paths. That is exactly why JJ2 is tectonically sensitive and could display a remarkable gas radon anomaly before the Ruichang-Yangxin M_L 5.0 earthquake in 2011. Our results also indicate that ascertaining the hydrological characteristics and cycling process of groundwater are crucial for understanding the earthquake anomalies and judging whether a seismic groundwater monitoring well is reliable or not.

KEYWORDS

hydrogeochemistry, stable isotope, tritium activity, geochemical characteristics, radon anomaly

1 Introduction

Underground fluid is proved to be an important carrier for transmitting information of geological evolution within the Earth and thus its geochemical characteristics and genesis are widely studied (Zhang, 1992; Che et al., 1998; Du and Kang, 2000; Liu, 2006; Li et al., 2022; 2023). Detailed researches involving the relationship between groundwater and surface runoff (Grasby et al., 1999; Su et al., 2009; Gu et al., 2017), the circulation process and water-rock interactions (He and Singh, 2019; Hosono and Masaki, 2020; Hosono et al., 2019; Nakagawa et al., 2020; Shi et al., 2020; Barberio et al., 2017; Skelton et al., 2014; Barberioet al., 2017; Zhou et al., 2020; Chen et al., 2015; Li et al., 2021; Martinelli and Dadomo, 2017; Skelton et al., 2019; Li et al., 2017; Bao et al., 2019; Du and Liu, 2003; Sun et al., 2016; Zhou et al., 2022; Tian et al., 2021; Song et al., 2006), the changes of chemical compositions before

FIGURE 1
(A) Structural geological map of the study area. **(B)** Schematic diagram of well structure and aquifers of JJ2. **(C)** Location of the study area.

and after earthquakes (Tsunogai and Wakita, 1995; Claesson et al., 2004; Reddy and Nagabhushanam, 2011; Reddy et al., 2011; He and Singh, 2019; Hosono and Masaki, 2020; Hosono et al., 2019; Nakagawa et al., 2020; Shi et al., 2020; Barberio et al., 2017; Skelton et al., 2014; Barberioet al., 2017; Zhou et al., 2020; Chen et al., 2015; Zhao et al., 2023), and the earthquake anomaly verification (Liu and Ren, 2009; Zhang et al., 2014; Zhang et al., 2016; Zhou et al., 2021). All these studies demonstrated that making clear the origin and forming process of underground fluid is the prerequisite for identifying earthquake precursors (Li et al., 2022; 2023).

Ruichang-Yangxin M_L 5.0 earthquake, occurred on 10 September 2011, is one of the large earthquakes occurred in the central and eastern regions of China in recent years. About 1 month before the earthquake, radon in groundwater from Jiujiang well number 2 (herein after JJ2) increased rapidly, showing a remarkably high value anomaly. The reason that JJ2 can exhibit such anomaly could be the fact that JJ2 is a cold spring located on the fault zone with a moderate groundwater age as there is a hypothesis that neither young and old groundwater can reflect the change of the geochemical environment in the crust effectively while groundwater with moderate age is more able to show relatively complete abnormal forms before earthquakes (Pan and Gao, 2001). But to better understand the cause of this radon anomaly, more detailed works need to be done on the groundwater characteristics in the JJ2. Therefore, this paper attempts to give a reasonable explanation to the seismic hydrogeochemical characteristics of the well and the causes of the pre-earthquake anomaly of gas radon through the analysis results of hydrochemical composition, hydrogen and oxygen isotopes and well water dating. This would provide a scientific basis for further understanding the recharge cycle and anomaly formation in shallow wells on the fault zone and exploring the formation mechanism of gas radon anomaly in areas with few earthquakes

FIGURE 2
Time-series map of earthquakes above M_L 2.0 within 150 km of the Jiujiang seismic station.
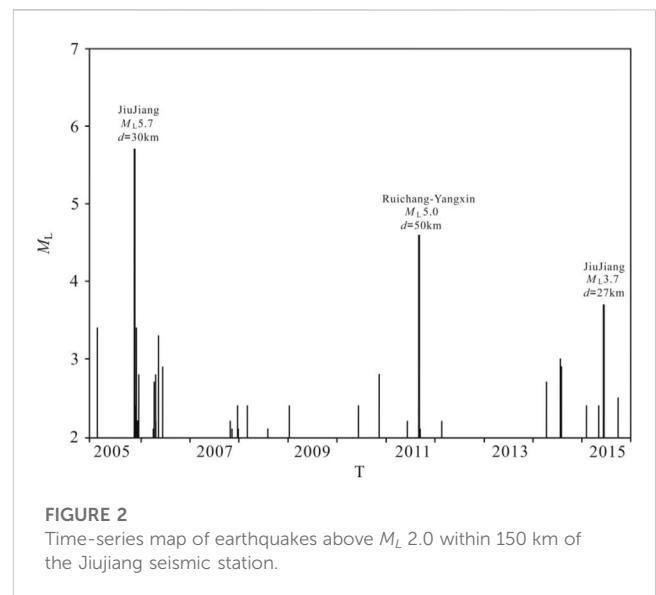
and weak earthquakes and its response relationship with regional tectonic activities.

2 Geological setting

The JJ2 is a typical well at the Jiujiang Seismic Monitoring Centre station (JJS) (29.65°N, 115.33°E, 110 m) which is located in the northwestern side of Lushan Mount (Mt Lushan) in the north of Jiangxi province and tectonically belongs to the junction zone of Yangtze block (Jiangnan ancient land) and Dabie Mountain block (Lv et al., 2008). The climate here is subtropical monsoon, with annual average temperature of 16.7°C and average annual precipitation of 1,300 mm. Active faults are well developed in the

area including the NE-trending Tanlu Fault, the NW-trending Xiangfan-Guangji Fault, and the NEE trending Xiajia-Weijialing Fault (Figure 1). The Xiajia-Weijialing fault near the JJ2 is a left strike-slip fault on the edge of the northwestern margin of Lushan Mountain. The fault extends for about 8 km wide and about 11.5 km long, with a general tendency 320°–330° and an inclination of 60~70°. The study area is seismically active, within which three earthquakes with magnitude above 3.0 have occurred since 2005, including the Jiujiang-Ruichang M_L 5.7 earthquake in 2005, the Ruichang-Yangxin M_L 5.0 earthquake in 2011, and the Jiujiang M_L 3.7 earthquake in 2015 (Figure 2).

JJ2 is a structurally confined artesian well started running since 2008. The well has the depth of 71 m and the casing of 11.9 m. From the surface to 6.2 m, it is composed of loam and gravel of Lianwei Formation of Quaternary; 6.2–11.9 m is composed of strongly weathered carbonaceous limestone of Piyuancun Formation of Sinian; and 11.9–71 m is composed of Lower Proterozoic carbonaceous limestone (Figure 1). The well has two aquifers at 17–22.5 m and 55–63.5 m respectively, and the current daily discharge is approximately 300 tons. There is a reservoir about 1 km away and a river about 50 m away which comes from the Maweishui (MWS) spring in the Mt Lushan.
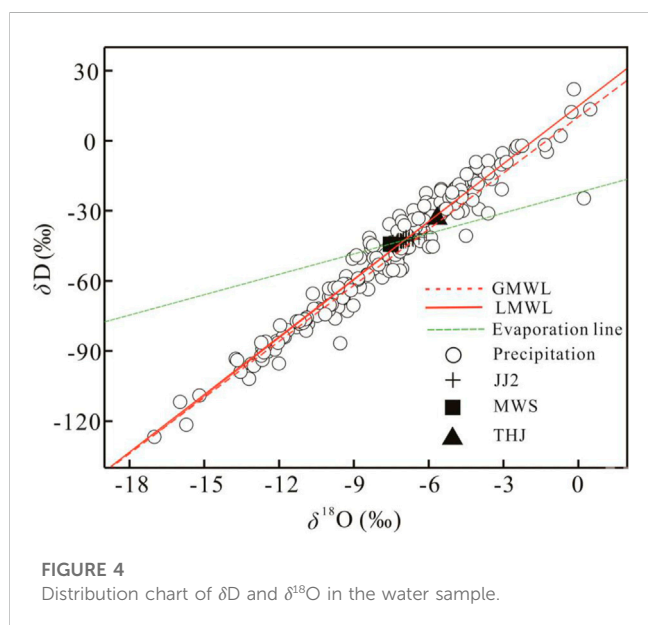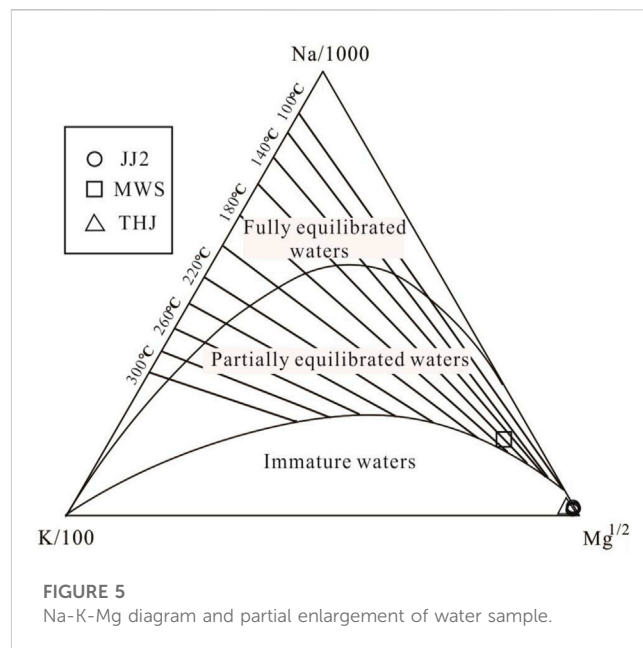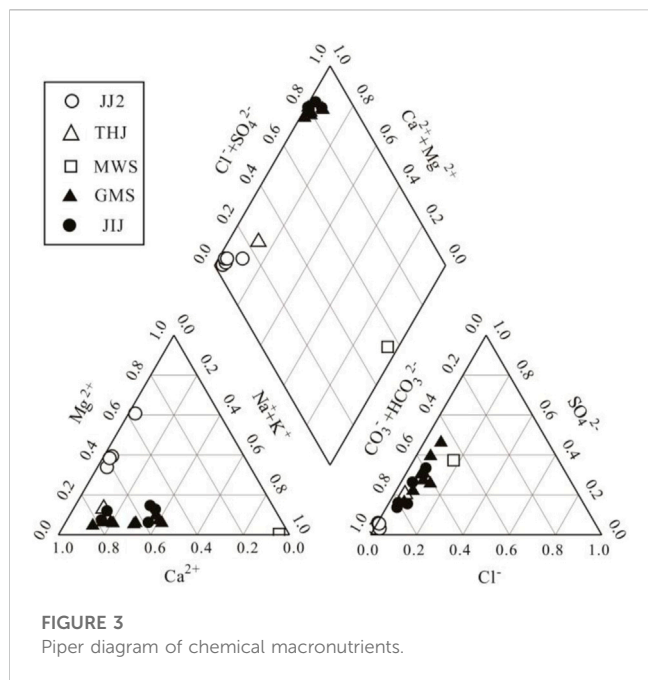
3 Sampling and analyzing methods

Atmospheric precipitations from the courtyard of JSS (JIJ), Guomiansichang (GMS), Xingang (XG), and Lushan Meteorological Bureau (LMB) were collected for δD and $δ^{18}O$ analysis. Water samples from the JJ2, MWS spring, and Tianhuajing reservoir (THJ) were collected for δD, $δ^{18}O$ and chemical analysis. The sampling bottle was high density polyethylene (HDPE) screw cap bottle with a thin neck. In order to avoid contamination of samples, sampling bottle was cleaned with deionized water before collecting samples, and then with the collected water sample for three times. By overflow method, the bottle was capped immediately after filling, and the mouth wrapped with parafilm. Two samples were collected at each sampling point. A total of 239 effective water samples were obtained, of which 198 were obtained from atmospheric precipitation, and 41 from JJ2, THJ reservoir and MWS spring water. The collection method was to connect a sampling bottle under the rain gauge. In order to prevent sundries from entering the sampling bottle, a ping-pong ball was placed in the rain gauge. Effective precipitation with long rainfall duration was used for test and analysis. Water samples from JJ2, which was used for hydrogen and oxygen isotope testing, were collected once every 2 weeks, and water samples from four different seasons were selected for hydrochemical composition analysis. The water from THJ reservoir and MWS spring were collected once for hydrogen and oxygen isotope and water chemical composition analysis. All samples were filtered through a 0.22 μm membrane before measurement.

Water temperature, pH value, and total dissolved solids (TDS) were recorded in the sampling point, and each parameter was measured thrice continuously and averaged. The hydrochemical components and hydrogen and oxygen isotope analysis of the samples were completed in the Key Laboratory of Crustal Dynamics (Underground Fluid Dynamics Laboratory Unit) of

TABLE 1 Summary of stable isotopes and chemical compositions of different water bodies in the Lushan regions ["-" represents no text data, "*" represents data from Bao et al. (2022)].

NO	Sample type	Longitude&altitude	Altitude (m)	temperature (°C)	TDS mg/L	pH	$δ^{18}O$ (‰)	δD (‰)	d (‰)	Na+	K+	Mg2+	Ca2+	F-	Cl-	SO42-	HCO3-	NO3-	Classify
JJ2	Well water	29.65°N,115.33°E	110	18.4	247.07~258.15	7.3	-7.42~-6.09	-43.87~-39.69	9.03~15.93	1.32~2.26	1.32~1.94	13.39~14.86	35.84~43.26	0.18~0.52	0.38~2.35	4.97~9.38	177.34~194.16	0.11~1.67	HCO3-Ca-Mg
JIJ	Precipitation	29.65°N,115.33°E	110	--	15.96~20.70	--	-12.45~-1.26	-90.30~-4.74	1.83~26.39	0.1~0.42	0.01~0.22	0.04~0.08	0.30~0.81	0.02~0.15	0.28~0.75	1.44~2.70	6.10~20.99	1.13~5.61	--
GMS	Precipitation	29.70°N,115.34°E	68	--	18.08~39.55	--	-10.65~-2.5	-65.4~-3.04	7.14~23.32	0.12~0.53	0.16~0.53	0.03~0.11	0.44~2.07	0.02~0.17	0.39~1.51	1.92~9.57	2.97~13.04	12.20	--
LMB	Precipitation	29.59°N,115.35°E	1325	--	--	--	-15.97~-0.48	-126.77~-22.11	-26.42~-25.53	--	--	--	--	--	--	--	--	--	--
XG	Precipitation	29.78°N,115.98°E	60	--	--	--	-13.00~-6.22	-96.13~-38.34	3.85~11.65	--	--	--	--	--	--	--	--	--	--
THJ*	Surface water	29.66°N,115.34°E	138	22.8	46.8	7.1	-5.66	-33.36	11.92	1.45	0.55	0.95	9.00	0.13	1.55	8.11	38.44	11.43	HCO3-Ca
MWS*	Spring	29.66°N,115.33°E	569	17.3	42.9	5.7	-7.53	-44.25	15.99	94.44	3.29	0.19	3.84	16.99	5.97	18.00	27.46	1.18	HCO3-Na

FIGURE 3
Piper diagram of chemical macronutrients.

FIGURE 5
Na-K-Mg diagram and partial enlargement of water sample.

FIGURE 4
Distribution chart of δD and δ18O in the water sample.

China Earthquake Administration, where major element analysis equipment used was ICS-2100 ion chromatograph (flow accuracy <0.1%). Oxygen isotope analysis equipment used was Picarro liquid water isotope analyzer (L2130-i type, United States of America), and the results of stable isotopes of hydrogen and oxygen were expressed in thousandths difference relative to Vienna standard mean marine water (VSMOW):

$$\delta = \left(R_{sample} - R_{standard} \right) / R_{standard} \times 1000 \quad (1)$$

Here, R_{sample} represents the ratio of $^{18}O/^{16}O$ (D/H) in the samples; $R_{standard}$ represents the ratio of $^{18}O/^{16}O$ (D/H) in VSMOW. The accuracy of the tests conducted was determined to be $\delta^{18}O < 0.05‰$ and $\delta D < 0.5‰$. The tritium isotope radioactivity of the samples was

tested at the Institute of Hydrogeology and Environmental Geology, Chinese Academy of Geological Sciences, using a Quantulus-1220 ultra-low background liquid scintillation spectrometer. Liquid scintillation counting was employed as the analytical method.

SD-3A Intelligent Digital Radon Meter operates based on the flashing light method. When radon gas enters the scintillation chamber, the α particles emitted from the decay of radon and its progeny cause the "fluorescent body" on the wall of the sampler in the scintillation chamber, which is made of ZnS (Ag), to emit weak flashes of light. The photomultiplier inside the instrument then detects and converts these flashes of light into electrical impulses. These electrical impulses are further amplified by the electronic circuits, and finally, the processor records the corresponding electrical impulse signals. Subsequently, the processor calculates the radon content (concentration) in the measured gas (or soil) using the principle of pulse count rate, which is determined by the number of electric pulses recorded per unit time.

4 Results

4.1 Hydrochemical characteristics

The main analytical phases of hydrochemistry in the study area (pH, TDS, Ca^{2+}, Mg^{2+}, Na^+, K^+, F^-, Cl^-, SO_4^{2-}, and HCO_3^-) are shown in Table 1. Generally, the pH values of groundwater and surface water were weakly alkaline, while that of MWS Spring was acidic. The TDS of JJ2 water, THJ water, and MWS water were 247.07~258.15 mg/L, 46.80 mg/L, and 42.90 mg/L respectively. The TDS of groundwater was higher than that of surface water. As can be seen in Piper's three-line diagram, the main positive ions include Ca^{2+}, Mg^{2+}, and Na^+, and the main negative ions are HCO_3^- and Cl^-. In the piper chart, the water samples are mainly distributed in three zones (Figure 3). Among them, the water samples on the first zone (JJ2 and THJ) belongs to the HCO_3–Ca·Mg type.
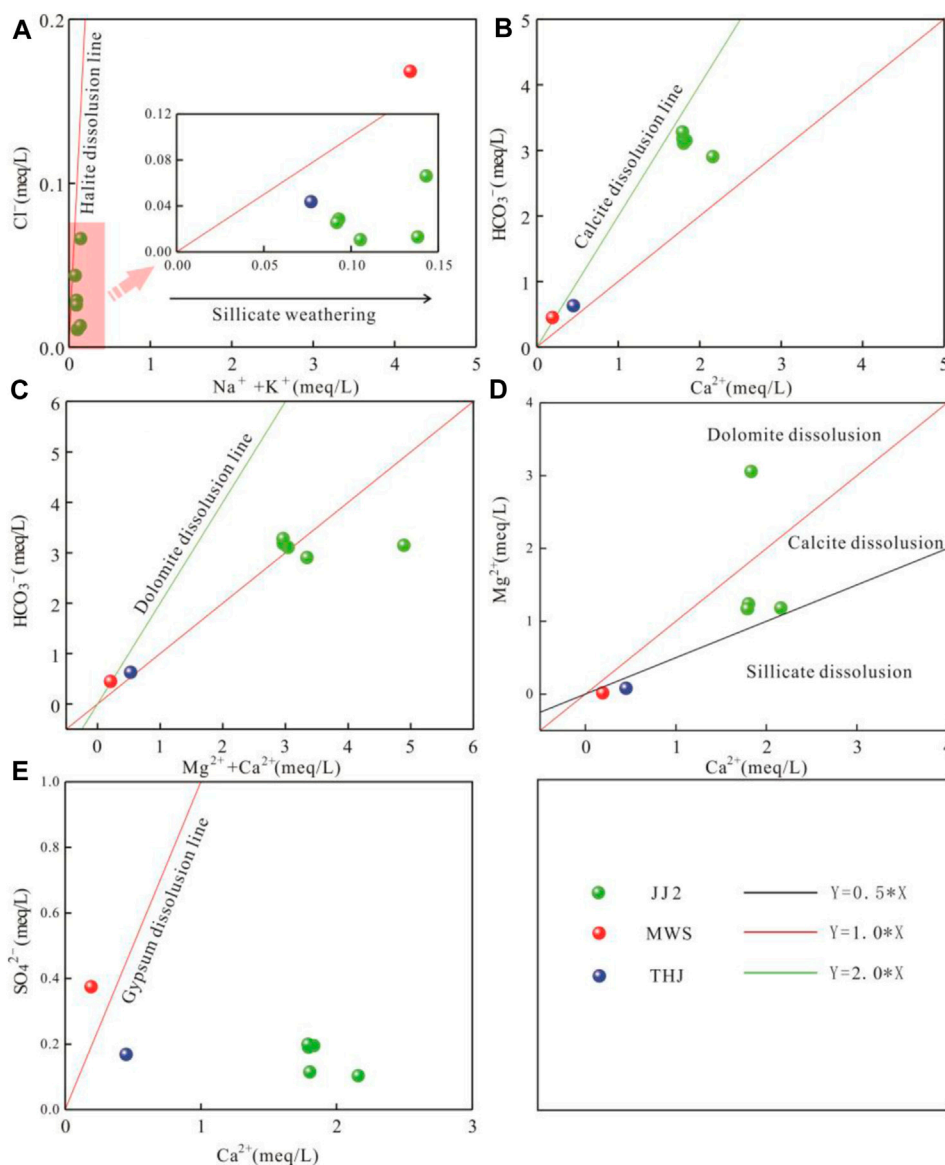
FIGURE 6
(A) Relationships between Na+ +K+ and Cl− of JJ2. **(B)** Relationships between Ca2+ and HCO3− of JJ2. **(C)** Relationships between Mg2+ +Ca2+ and HCO3− of JJ2. **(D)** Relationships between Ca2+ and Mg2+of JJ2. **(E)** Relationships between Ca2+ and SO4²−of JJ2.

Atmospheric precipitations (JIJ and GMS) in the second zone belongs to the Cl–Na type. Other water samples are located in the third zone of the piper diamond graph that belong to the HCO_3–Na type.

4.2 Characteristics of hydrogen and oxygen isotope composition

The measured values of hydrogen isotope (δD) and oxygen isotope isotopic composition (δ^{18}O) in JJ2 was −43.87‰~-39.69‰ and −7.42‰~-6.09‰, respectively. The mean values of δ^{18}O and δD for the JJ2 are −6.99‰ and −42.55‰ respectively. The measured value of δD and δ^{18}O in atmospheric precipitation was −126.77‰ ~22.11‰ and-15.97‰~0.48‰, respectively. The mean values of δ^{18}O and δD for the atmospheric precipitation are −7.67‰

and −48.68‰ respectively. According to the measured values of hydrogen and oxygen isotopes of atmospheric precipitation, the local atmospheric precipitation line was: δD=8.6 δ^{18}O+18.8 (r=0.97, n= 198), and the slope and intercept were roughly the same as those in Nanjing (Wang et al., 2013; Liu et al., 2014). According to the δD and δ^{18}O of groundwater in JJ2, the evaporation line of groundwater at JJS was fitted as: δD= 3.0 δ^{18}O-21.9 (r=0.86, n=34). Moreover, it could be observed that δD and δ^{18}O of the JJ2 water are mainly distributed near the meteoric water line (Figure 4). Compared with the local precipitation line and the global atmospheric precipitation line, the slope and intercept of the fitted evaporation line were obviously smaller, which indicates that the whole water belongs to the atmospheric genetic type and experienced certain evaporation before the atmospheric precipitation is replenished (Craig, 1961; Giggenbach, 1992).
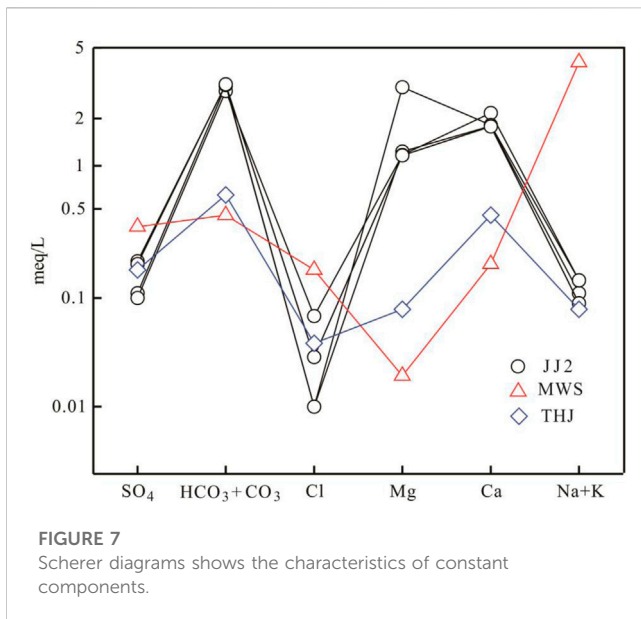
FIGURE 7
Scherer diagrams shows the characteristics of constant components.

4.3 Gas radon concentrations

The intelligent digital radon-detectors (SD-3A) samples once every hour. This paper provides the observed gas radon data time series from January to December 2011 (Figure 9C). It can be seen that the normal background values are varying in range of 0.3 Bq/L to 2.0 Bq/L. However, the value began to rise rapidly since 12th of August 2011 and reach a maximum value of 28.5Bq/L on 30th of August. After that, the value began to decline. During the process, the Ruichang-Yangxin M_L5.0 earthquake occurred on 11 September, which is about 27 km away from the JJ2.

5 Discussion

5.1 Groundwater circulation depth

Groundwater geochemical evolution is mainly controlled by various chemical reactions between water and rock, and identifying these reactions is the basis of groundwater geochemical evolution research (Giggenbach, 1988). In this paper, Na-K-Mg triangle graphic method is utilized to analyze the chemical equilibrium reaction characteristics and cycle depth of groundwater components. The Na–K–Mg triangular plot (Figure 5) shows the sample of JJ2 and THJ are in immature water zone, indicating that they are not fully equilibrated with the reservoir rocks. The sample of MWS plot in the partial equilibrated water zone, which show that part of water-rock interaction had reached equilibrium, the circulating depth of underground water was deep.

Cation geothermometers can be used to estimate approximate reservoir temperatures. In this study, the Na-K-Mg triangulation based on Na-K and K-Mg geothermometers were used to assess the thermal storage temperature of underground water samples. According to the temperature marking in Figure 5, the reservoir temperatures of groundwater in JJ2 was about 60~80 °C, and the MWS sample was about 160°C.

According to the reservoir temperature, the circulated depth calculation formula shown as follows is adopted

$$Z = Z_0 + (T - T_0)\big/T_{grad} \qquad (2)$$

Here, Z represents the circulation depth (km); Z_0 represents the depth of the constant temperature zone (km); T represents the reservoir temperature (°C); T_0 represents the temperature of the constant temperature zone (°C), namely, the local average temperature; Tgrad represents the geothermal gradient (°C/km) reflecting the geothermal change per kilometer of the place below the constant temperature zone (Xiong et al., 1990). Based on the previous studies on groundwater in the study area, we selected the geothermal gradient Tgrad of 21.3°C/km (Wang et al., 2023a), the annual mean temperature T_0 in the Jiujiang is 17.5°C, and the Z_0 is 20 m. The circulation depth of the JJ2 and MWS are about 2015~2,954 m and 6710 m respectively, which implies that the circulating path of groundwater in MWS spring was different from that in JJ2. The circulation depth and the reservoir temperature of the JJ2 and MWS are positive-related. Cool waters are likely involved during the long circulation pathways between the reservoir and the spring vent.

5.2 Recharge elevation

The linear regression between different elevations and their hydrogen and oxygen isotope ratios could fit the elevation gradient of oxygen isotopes in the study area. When studying the groundwater recharge elevation, "isotope elevation gradient" can be used in a local area. According to previous research results (Ou et al., 2011), the elevation gradient of δ^{18}O and δD in Lushan area is 0.188‰/100 m and 0.0138‰/100 m respectively. The recharge elevation of groundwater in the study area can be estimated by using the elevation gradient value, and its calculation formula is as follows:

$$H = \frac{(\delta G - \delta P)}{K} + h \qquad (3)$$

Here, H represents the recharge elevation (m), h represents the sampling point elevation (m); δ_G represents the isotopic composition of underground water (‰), δ_P represents the atmospheric precipitation near the sampling point (‰); K represents the isotopic altitude gradient (‰/100 m). Considering the probably oxygen drift caused by water-carbonate rock interaction (Pang et al., 2017), $K_{\delta D} = 0.0138‰/100$ m was used in this study. So, the calculated recharge elevation calculated is 554 m.

5.3 Groundwater age

Tritium is a radioactive isotope of hydrogen, with a half-life of 12.43 a (Lucas and Unterweger, 2000), which can be subdivided into natural tritium and artificial tritium according to its origin. Natural tritium mainly comes from cosmic rays, and artificial tritium mainly comes from human activities such as nuclear experiments. Tritium is released during the month of precipitation, surface water, and groundwater, and is not easy to react with environmental media along with hydrogeological and other processes for life, but only follows the radioactive law, with the change being quite independent (Wang, 1991). Based on the inherent characteristics of tritium, it

FIGURE 8
(A) Schematic diagram of the observation well. **(B)** The source of escaping gas radon.
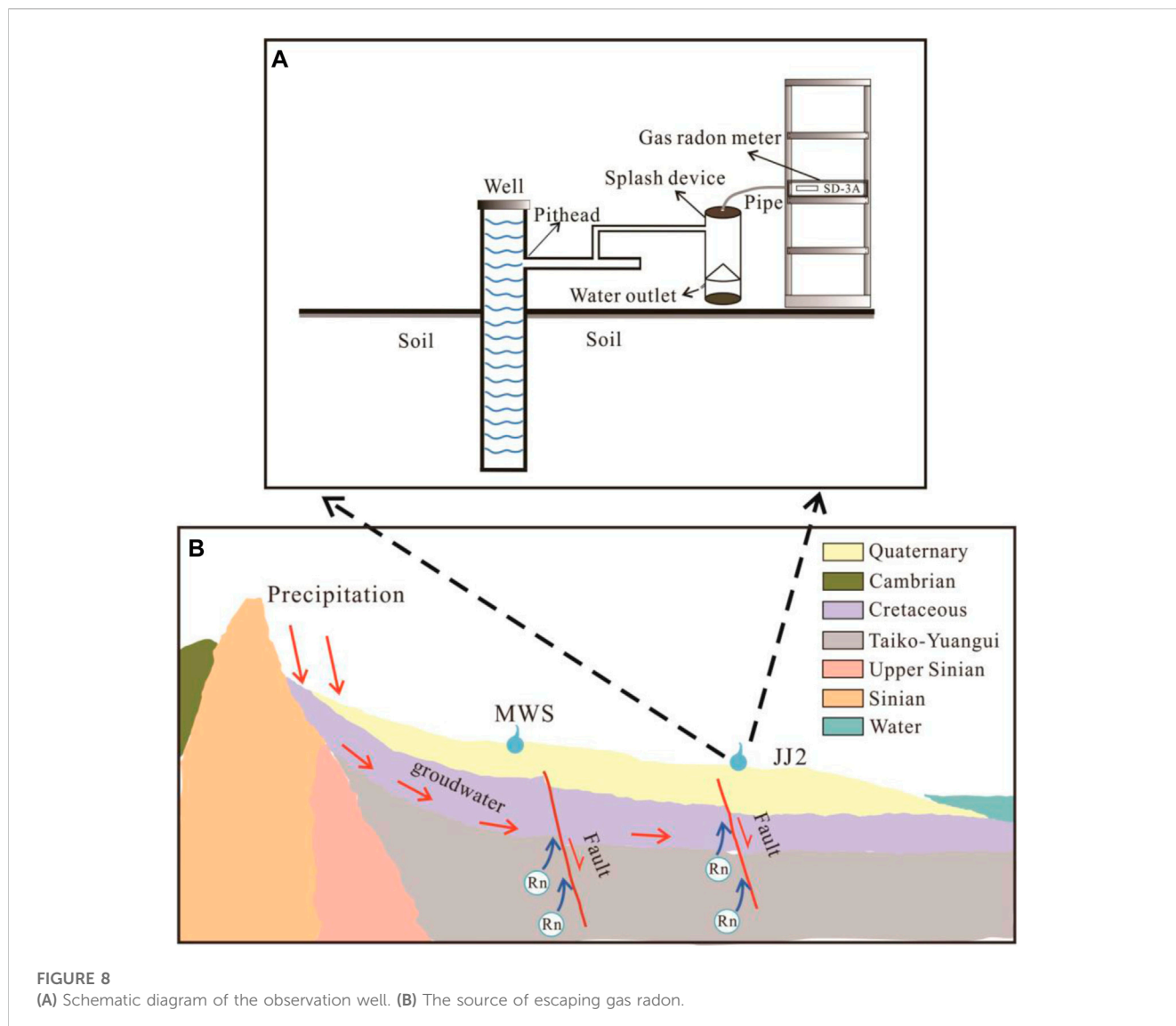
tends to estimate the age of groundwater and discriminate the source of recharge. The tritium content in the natural state is very low (<0.5). According to previous studies (Gu, 2011), when the activity is less than 1.0 Tritium Unit (TU), the old water was replenished before 1953, 1~3 TU, old water mixed with new water for nearly 10 years. According to recent study, the tritium activity of JJ2 is 1.6 ± 0.6TU (Bao et al., 2022), which indicated that the JJ2 has both old water supply and nearly 10 years new water supply, the groundwater was of moderate age and had the conditions to reflect the dynamic changes of medium and environment in the fault zone (Zhang et al., 2019). It also implied that the two aquifers in JJ2 have different circulation paths and recharge sources.

5.4 Petrographic compositions involved in dissolution and hydraulic relationship

The ratio of ion molar concentrations in groundwater is often used to discriminate the source of dissolved ionic minerals in the water samples (Su et al., 2022). $\gamma Cl/\gamma Na+K$ ratios of most waters

fall below 1:1 ratio line (Figure 6A), implying that cation exchange and weathering of silicates ($NaAlSi_3O_8+8H_2O \rightarrow Na^+ + Al(OH)_4 + 3H_4SiO_4$) may be significant processes along the JJ2 (Xiao et al., 2022; Wang et al., 2023b). As shown in Figures 6B, C, $\gamma HCO_3/\gamma Ca$ in the waters of JJ2 fall in the zone between lines 1: 1 and 1:2, and the ratio of $\gamma HCO_3/\gamma Mg+Ca$ in all waters of JJ2 mostly fall along the line 1:1, combined with the chemical types of HCO_3-Ca·Mg in JJ2, suggesting that the dissolution of calcite and dolomite are relevant to the lixiviation of carbonate. This phenomenon is also consistent with the lithological characteristics of the strata around JJ2. As shown in Figure 1, the stratigraphic lithology around the aquifer of JJ2 consists of carbonaceous greywacke, siliceous greywacke and sandstone, constituted mainly by calcites, dolomites, quartz, feldspars and clay minerals. So, Ca^{2+} and Mg^{2+} mainly originate from the dissolution of carbonates (calcites and dolomites), as well as some silicate minerals such as feldspars, which is further evidenced by the results in Figure 6D where the JJ2 samples fall mainly in the calcite dissolution zone, and occasionally in the dolomite dissolution zone.
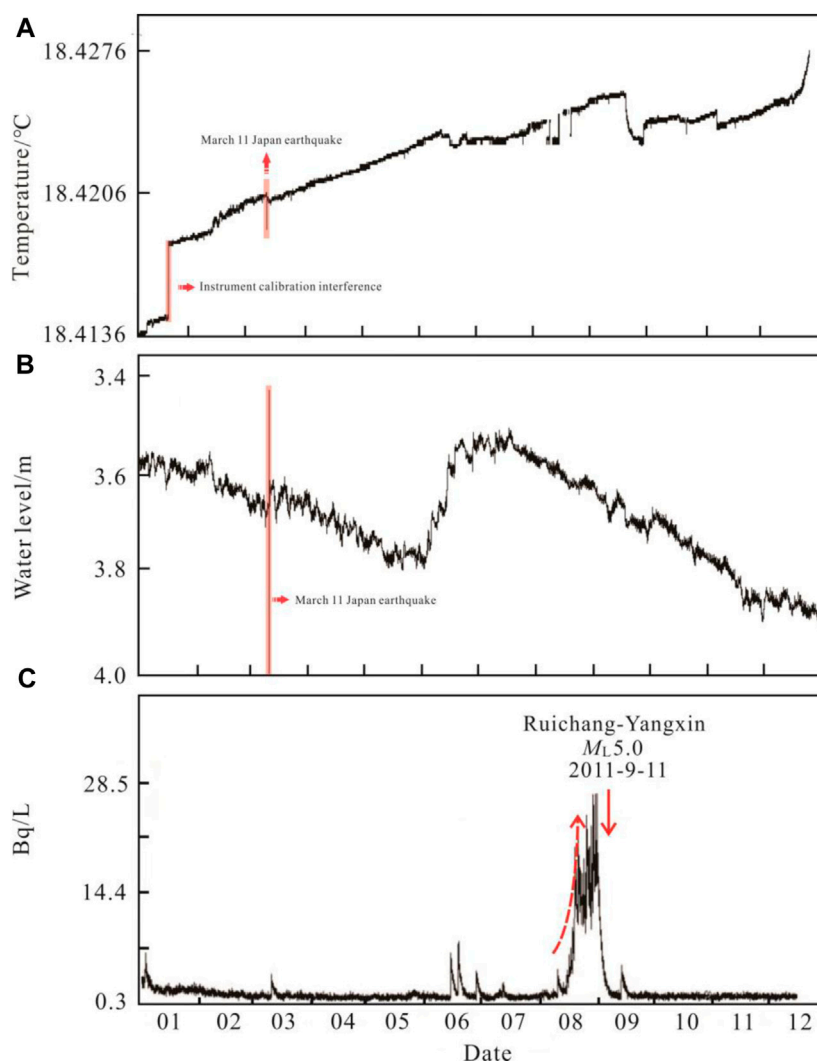
FIGURE 9
(A) Time series diagram of water temperature from JJ2. **(B)** Time series diagram of water level from JJ2. **(C)** Time series diagram of gas radon concentration from JJ2.

Scherer diagram can intuitively reflect the chemical characteristics of different water bodies. It is generally believed that waters with strong morphological consistency may have similar sources and circulation processes. Therefore, Scherer diagrams are often used to distinguish the hydraulic relationships of different water bodies. (Craig, 1961; Zhang et al., 2019). As shown in Figure 7, it can be found that the ion sources of MWS and THJ are more complex compared to JJ2, in which MWS mainly includes calcite, dolomite, silicate and gypsum, while THJ mainly include calcite, dolomite, silicate, gypsum and Halite. The ion content curves of MWS and JJ2 are significantly different from each other, suggesting that they are not hydraulically connected. In the piper diagrams (Figure 3), the water of JJ2 and MWS belong to different water chemistry types, which further implies that they have different origins. Although the hydrochemistry types of JJ2 and THJ are the same, the morphology of their ion content curves are still very

different, so it is discriminate that they are weakly hydraulically connected to each other. This is similar to the results reflected in Figure 6.

5.5 Response of observation well to seismic activity

The evolution of d excess of groundwater is mainly controlled by surrounding rocks, oxygen-bearing components, lithology and aquifer sealing conditions, water retention time, and physical and chemical properties of water. The d value of JJ2 was 9.03~15.93, with the mean value of 13.40, which belongs to modern circulating leaching water (Bao et al., 2021). This is consistent with the fact that JJ2 samples are located in the immature area of the Na-K-Mg block, and have a shallow recharging elevation. That is to say, JJ2's aquifer cycle

recharge faster and do not react adequately with the surrounding rocks. The δD and δ^{18}O compositions indicates that the source of water in JJ2 is of the atmospheric precipitation genesis type, so the main recharge source of water in the aquifer in JJ2 is the atmospheric precipitation via infiltration through the rock fissures (Figure 8C). However, some deep-derived fluids may also get involved as evidenced by the results of the tritium activity analysis.

Radon, as an earthquake-sensitive component of subsurface fluids, is one of the longest observed and most widely used monitoring items in the field of earthquake forecasting. Abundant studies have proved that there are significant Rn anomalies before the occurrence of earthquakes (Igarashi et al., 1995; Sugisaki et al., 1996; Liu and Ren, 2009; Muto et al., 2021). One month before the Ruichang-Yangxin M_L 5.0 earthquake (<50 km), escaping radon in JJ2 showed significant high value anomalies (Figure 9C). Based on the results above, we think that there are two reasons resulting such sensitive response. Firstly, the JJ2 is located right on the fault, so its aquifer is connected well to the fault fracture zone which provides abundant pathways for circulation of substances in the underground fluid in the preparation process of earthquakes (Figure 8A); Secondly, the JJ2 is fed by moderate aged water, which can promptly reflect the changes in the geochemical environment within the earth's crust and show a more complete pattern of anomaly before the earthquake. In addition, the water level and water temperature measurements in the observation wells did not observe obvious precursor anomalies before the earthquakes (Figures 9A, B), indicating that the hydrophysical observations were not sensitive or the sensitivity of the instruments was not enough to capture the significant anomalies.

6 Conclusion

In this study, the water samples from the JJ2 well, THJ reservoir, MWS spring, and local atmospheric precipitations were collected and analyzed, based on which responding mechanism of water in JJ2 to tectonic activities were discussed. Main conclusions were obtained as follows:

(1) The water type of the JJ2 and THJ is HCO$_3$-Ca-Mg type, and of MWS spring is HCO$_3$-Na type. The JJ2 water experienced weak water-rock interactions and belongs to the immature water, with the circulating depth of 2015~2,954 m. MWS spring water experienced relative more intense water-rock interactions and is close to the partially equilibrated water, having the circulating depth about 6710 m. In addition, the waters from the JJ2, MWS spring, and THJ reservoir are not hydraulically connected.

(2) The JJ2 water is mainly a modern leaching water of atmospheric origin, with recharge elevation of about 554 m, and partially exchanged with fluids from deep parts of the fault.

(3) Due to the JJ2 is located right on the fault and has characteristics of both shallow and deep circulating water, JJ2 water can respond to regional tectonic activities sensitively as evidenced by the Radon anomaly before the Ruichang-Yangxin M_L 5.0 earthquake in 2011.

Data availability statement

The original contributions presented in the study are included in the article/supplementary material, further inquiries can be directed to the corresponding author.

Author contributions

ZB: Investigation, Methodology, Writing–original draft. LH: Conceptualization, Funding acquisition, Writing–review and editing. JX: Investigation, Writing–original draft. XZ: Investigation, Methodology, Writing–original draft. JL: Data curation, Investigation, Writing–original draft. YZ: Investigation, Writing–original draft.

Conflict of interest

The authors declare that the research was conducted in the absence of any commercial or financial relationships that could be construed as a potential conflict of interest.

The reviewer XZ declared a shared affiliation with the author LH to the handling editor at time of review.

Publisher's note

All claims expressed in this article are solely those of the authors and do not necessarily represent those of their affiliated organizations, or those of the publisher, the editors and the reviewers. Any product that may be evaluated in this article, or claim that may be made by its manufacturer, is not guaranteed or endorsed by the publisher.

References

Bao, Z., Gao, X., Zhang, L., Zhao, Y., Zha, X., Xiang, Y., et al. (2019). Hydrogen and oxygen isotope characteristics and significance of groundwater from Jiu-jiang seismic station. *Earthq. Res. China* 35, 499–508. (In Chinese).

Bao, Z., Zha, X., Gao, X., Zhao, Y., Zhao, A., Xu, Z., et al. (2022). Hydrogeochemincal characteristics and genesis for jiujiang NO.2 well in Jiangxi Province. *China Earthq. Eng. J.* 44, 920–928. (In Chinese). doi:10.20000/j.1000-0844.20210201001

Bao, Z., Zha, X., Zhao, Y., Zhao, A., Xiang, Y., and Jiang, Y. (2021). Hydrogeochemical characteristics and genesis of groundwater in Lushan area of Jiujiang. *J. Geodesy Geodynameics* 41, 471–477. (In Chinese). doi:10.14075/j.jgg.2021.05.006

Barberio, M. D., Barbieri, M., Billi, A., Doglioni, C., and Petitta, M. (2017). Hydrogeochemical changes before and during the 2016 Amatrice-Norcia seismic sequence (central Italy). *Sci. Rep.* 7, 11735. doi:10.1038/s41598-017-11990-8

Che, Y., Liu, W., and Yu, J. (1998). The relationship between crustal fluids and major earthquakes and its implications for earthquake prediction. *Seismol. Geol.* 20, 431–436. (In Chinese). doi:10.1088/0256-307X/16/9/027

Chen, Z., Zhou, X., Du, J., Xie, C., Liu, L., Li, Y., et al. (2015). Hydrochemical characteristics of hot spring waters in the Kangding district related to the Lushan <i&gt;M&lt;/i&gt;<sub&gt;S&lt;/sub&gt; = 7.0 earthquake in Sichuan, China. *Nat. Hazards Earth Syst. Sci.* 15, 1149–1156. doi:10.5194/nhess-15-1149-2015

Claesson, L., Skelton, A., Graham, C., Dietl, C., Mörth, M., Torssander, P., et al. (2004). Hydrogeochemical changes before and after a major earthquake. *Geology* 32, 641–644. doi:10.1130/g20542.1

Craig, H. (1961). Isotopic variations in meteoric waters. *Science* 133, 1702–1703. doi:10.1126/science.133.3465.1702

Du, J., and Kang, C. (2000). Characteristics of earthquake precursors and its geological significance. *Earthquake* 20, 95–101. (In Chinese). doi:10.3969/j.issn.1000-3274.2000. 03.015

Du, J., and Liu, C. (2003). Isotopic-geochemical application to earthquake prediction. *Earthquake* 23, 274–279. (In Chinese). doi:10.3969/j.issn.1000-3274.2003.02.012

Giggenbach, W. F. (1988). Geothermal solute equilibria:Derivation of Na-K-Mg-Ca geoindicators. *Geochim. A. T. Cosmochim. Acta* 52, 2749–2765. doi:10.1016/0016-7037(88)90143-3

Giggenbach, W. F. (1992). Isotopic shifts in waters from geothermal and volcanic systems along convergent plate boundaries and their origin. *Earth Planet. Sci. Lett.* 113, 495–510. doi:10.1016/0012-821x(92)90127-h

Grasby, S. E., Hutcheon, L., and McFarland, L. (1999). Surface-water-groundwater interaction and the influence of ion exchange reactions on river chemistry. *Geology* 27, 223–226. doi:10.1130/0091-7613(1999)027<0223:swgiat>2.3.co;2

Gu, H., Chi, B., Wang, H., Zhang, Y., and Wang, M. (2017). Relationship between surface water and groundwater in the Liujiang Basin—hydrochemical constrains basin-hydrochemical Constrains. *Adv. Earth Sci.* 32, 789–799. (In Chinese). doi:10.11867/j.issn.1001-8166.2017.08.0789

Gu, W. (2011). *Isotope hydrology*. Beijing, China: Science Press. (In Chinese).

He, A., and Singh, R. P. (2019). Coseismic groundwater temperature response associated with the wenchuan earthquake. *Pure Appl.Geophys.* 177, 109–120. doi:10. 1007/s00024-019-02097-4

Hosono, T., and Masaki, Y. (2020). Post-seismic hydrochemical changes in regional groundwater flow systems in response to the 2016 Mw 7.0 Kumamoto earthquake. *J. Hydrol.* 582, 124340. doi:10.1016/j.jhydrol.2019.124340

Hosono, T., Yamada, C., Shibata, T., Tawara, Y., Wang, C. Y., Manga, M., et al. (2019). Coseismic groundwater drawdown along crustal ruptures during the 2016 Mw 7.0 Kumamoto earthquake. *Water Resour. Res.* 55, 5891–5903. doi:10.1029/2019wr024871

Igarashi, G., Saeki, S., Takahata, N., Sumikawa, K., Tasaka, S., Sasaki, Y., et al. (1995). Ground-water radon anomaly before the kobe earthquake in Japan. *Science* 269 (5220), 60–61. doi:10.1126/science.269.5220.60

Li, C., Zhou, X., Yan, Y., Quyang, S., and Liu, F. (2021). Hydrogeochemical characteristics of hot springs and their short-term seismic precursor anomalies along the xiaojiang fault zone, southeast tibet plateau. *Water* 13, 2638. doi:10.3390/w13192638

Li, J., Li, Y., Lu, L., Sun, F., Xie, C., and Cui, Y. (2017). Geochemistry of sping water in the liupan mountain area. *Earthquake* 37, 61–72. (In Chinese). doi:10.3969/j.issn.1000-3274.2017.01.007

Li, Y., Chen, Z., Hu, L., Su, S., Zheng, C., Liu, Z., et al. (2022). Advances in seismic fluid geochemistry and its application in earthquake forecasing. *Chin. Sci. Bull.* 67, 1404–1420. (In Chinese). doi:10.1360/TB-2021-0955

Li, Y., Fang, Z., Zhang, C., Li, J., Bao, Z., Zhang, X., et al. (2023). Research progress and prospect of seismic fluid geochemistry in short-imminent earthquake prediction. *Seismol. Geol.* 45 (3), 593621. (In Chinese). doi:10.3969/j.issn.0253-4967.2023.03.001

Liu, J., Song, X., Yuan, G., Sun, X., and Yang, L. (2014). Stable isotopic compositions of precipitation in China. *Tellus Ser. B-Chemical Phys. Meteorology* 66, 22567. doi:10.3402/tellusb.v66.22567

Liu, L., Chen, H., Yang, Y., and Wang, J. (2008). Characteristics and genesis of rNa/rCl in shallow groundwater in the Suzhou-Wuxi-Changzhou region. *Geol. China* 35, 117–122. (In Chinese). doi:10.3969/j.issn.1000-3657.2008.01.012

Liu, Y. (2006). Review of the research progress on the seismological science of underground fluid in China during Last 40 Years. *Earthq. Res. China* 22, 222–235. (In Chinese). doi:10.3969/j.issn.1001-4683.2006.03.002

Liu, Y., and Ren, H. (2009). Preliminary analysis of the characteristics of post-seismic effect of radon after the wenchuan 8 .0 earthquake. *Earthquake* 29 (1), 12–131. (In Chinese). doi:10.3969/j.issn.1000-3274.2009.01.016

Liu, Y., Ren, H., and Wang, B. (2009). Application prospect of environmental isotopes and tracing techniques for earthquake prediction. *Earth Sci. Front.* 16, 369–377. (In Chinese). doi:10.1016/s1872-5791(08)60076-7

Lucas, L., and Unterweger, M. (2000). Comprehensive review and critical evaluation of the half-life of tritium. *J. Res. Natl. Inst. Stand. Technol.* 105, 541–549. doi:10.6028/jres.105.043

Lv, J., Zheng, Y., Ni, S., and Gao, J. (2008). Focal mechanisms and seismogenic structures of the M$_S$ 5.7 and M$_S$ 4.8 Jiujiang-Ruichang earthquakes of Nov. 26, 2005. *Chin. J. Geophys.* 51, 158–164. (In Chinese). doi:10.3321/j.issn:0001-5733.2008.01.020

Martinelli, G., and Dadomo, A. (2017). Factors constraining the geographic distribution of earthquake geochemical and fluid-related precursors. *Chem. Geol.* 469, 176–184. doi:10.1016/j.chemgeo.2017.01.006

Muto, J., Yasuoka, Y., Miura, N., Iwata, D., Nagahama, H., Hirano, M., et al. (2021). Preseismic atmospheric radon anomaly associated with 2018 Northern Osaka earthquake. *Sci. Rep.* 11 (1), 7451. doi:10.1038/s41598-021-86777-z

Nakagawa, K., Yu, Z. Q., Berndtsson, R., and Hosono, T. (2020). Temporal characteristics of groundwater chemistry affected by the 2016 Kumamoto earthquake using self-organizing maps. *J. Hydrol.* 582, 124519. doi:10.1016/j.jhydrol. 2019.124519

Ou, Y., Zhong, J., Liao, J., Yu, M., and Yin, R. (2011). Discussion on geothermal water in lushan xingzi hot spring. *J. East China Inst. Technol.* 34, 81–85. (In Chinese). doi:10. 3969/j.issn.1674-3504.2011.01.013

Pan, S., and Gao, A. (2001). A preliminary study on the relation between reflecting earthquake ability of spring and groundwater age and its application in earthquake prediction. *Northwest. Seismol. J.* 23, 189–193. (In Chinese). doi:10.3969/j.issn.1000-0844.2001.02.017

Pang, Z., Kong, Y., Li, J., and Tian, J. (2017). An isotopic geoindicator in the hydrological cycle. *Procedia Earth and Planetary Science* 17, 534–537. doi:10.1016/j.proeps.2016.12.135

Qiu, X., Wang, Y., Wang, Z., Regenauer-Lieb, K., Zhang, K., and Liu, J. (2018). Determining the origin, circulation path and residence time of geothermal groundwater using multiple isotopic techniques in the Heyuan Fault Zone of Southern China. *J. Hydrology* 567, 339–350. doi:10.1016/j.jhydrol.2018.10.010

Reddy, D., and Nagabhushanam, P. (2011). Groundwater electrical conductivity and soil radon gas monitoring for earthquake precursory studies in Koyna, India. *Appl. Geochmistry* 26, 731–737. doi:10.1016/j.apgeochem.2011.01.031

Reddy, D., Nagabhushanam, P., and Sukhija, B. S. (2011). Earthquake (M$_S$ 5.1) induced hydrogeochemical and δ^{18}O changes: validation of aquifer breaching-mixing model in koyna, India. *Geophys. J. Int.* 184, 359–370. doi:10.1111/j.1365-246x.2010. 04838.x

Shi, Z., Zhang, H., and Wang, G. (2020). Groundwater trace elements change induced by M5.0 earthquake in Yunnan. *J. Hydrol.* 581, 124424. doi:10.1016/j.jhydrol.2019. 124424

Skelton, A., Andrén, M., Kristmannsdóttir, H., Stockmann, G., Mörth, C. M., Sveinbjörnsdóttir, Á., et al. (2014). Changes in groundwater chemistry before two consecutive earthquakes in Iceland. *Nat. Geosci.* 7, 752–756. doi:10.1038/ngeo2250

Skelton, A., Claesson, L. L., Wästeby, N., Andrén, M., Stockmann, G., Sturkell, E., et al. (2019). Hydrochemical changes before and after earthquakes based on long-term measurements of multiple parameters at two sites in northern Iceland—a review. *J. Geophys. Res. Solid Earth.* 124, 2702–2720. doi:10.1029/2018jb016757

Song, S., Ku, W., Chen, Y., Liu, C., Chen, H., Chan, P., et al. (2006). Hydrogeochemical anomalies in the springs of the chiayi area in west-central taiwan as possible precursors to earthquakes. *Pure Appl. Geophysics* 163, 675–691. doi:10.1007/s00024-006-0046-x

Su, C., Nie, F., Zou, S., Zhao, G., Lu, F., Huang, Q., et al. (2018). Hydrochemical characteristics and formation mechanism of strontium-rich groundwater in xintian county, hunan province. *Geoscience* 32, 554–564. (In Chinese). doi:10.19657/j.geoscience.1000-8527.2018.03.13

Su, S., Li, Y., Chen, Z., Chen, Q., Liu, Z., Lu, C., et al. (2022). Geochemistry of geothermal fluids in the zhangjiakou-penglai fault zone, north China: implications for structural segmentation. *J. Asian Earth Sci.* 230, 105218. doi:10.1016/j.jseaes.2022. 105218

Su, X., Wan, Y., Dong, W., and Hou, G. (2009). Hydraulic relationship between malianhe river and groundwater: hydrogeochemical and isotopic evidences. *J. Jilin*

Univ. (Earth Sci. Ed. 39, 1087–1094. (In Chinese). doi:10.3969/j.issn.1671-5888.2009.06.017

Sugisaki, R., Takamoriito, I., Nagamine, K., and Kawabe, I. (1996). Gas geochemical changes at mineral springs associated with the 1995 southern Hyogo earthquake (M = 7.2), Japan. *Jpn. Earth Planet. Sci. Lett.* 139, 239–249. doi:10.1016/0012-821x(96)00007-6

Sun, X., Wang, G., Shao, Z., and Si, X. (2016). Geochemical characteristics of emergent gas and groundwater in Haiyuan fault zone. *Earth Sci. Front.* 23, 140–150. (In Chinese). doi:10.13745/j.esf.2016.03.018

Tian, J., Li, Y., Zhou, X., Peng, Z., Li, L., Xing, L., et al. (2021). Geochemical characteristics of hydrothermal volatiles from southeast China and their implications on the tectonic structure controlling heat convection. *Front. Earth Sci.* 9, 786051. doi:10.3389/feart.2021.786051

Tsunogai, U., and Wakita, H. (1995). Precursory chemical changes in groundwater: kobe earthquake, Japan. *Science* 269, 61–63. doi:10.1126/science.269.5220.61

Wang, A., Sun, Z., Lan, W., Yang, N., Ye, H., Tong, Y., et al. (2023a). Occurrence features of geothermal resources and geothermal potential assessment of Jiangxi Province. https://kns.cnki.net/kcms2/detail/11.1167.P.20230728.1454.002.html.

Wang, H. (1991). *Introduction to isotope hydrogeology*. Peking: Geological Publishing House, 30–50.

Wang, T., Zhang, J., Liu, X., and Yao, L. (2013). Variation of stable isotopes in precipiation and water vapor sources in Nanjin Area. *J. China Hydrology* 33, 25–31. (In Chinese). doi:10.3969/j.issn.1000-0852.2013.04.005

Wang, Y., Yuang, X., Zhang, Y., Zhang, X., Xiao, Y., Duo, J., et al. (2023b). Hydrochemical, D–O–Sr isotopic and electromagnetic characteristics of geothermal waters from the Erdaoqiao area, SW China: insights into genetic mechanism and scaling potential. *Ore Geol. Rev.* 158, 105486. doi:10.1016/j.oregeorev.2023.105486

Xiao, Y., Liu, K., Hao, Q., Xiao, D., Zhu, C., Yin, S. Y., et al. (2022). Hydrochemical insights into the signatures, genesis and sustainable perspective of nitrate enriched groundwater in the piedmont of Hutuo watershed, China. *Catena* 212, 106020. doi:10.1016/j.catena.2022.106020

Xiong, L., Wang, J., and Pang, Z. (1990). Circulation depth of the thermal water in Zhangzhou geothermal fifield. *Sci. Geol. Sin.* 4, 377–384. (In Chinese).

Zhang, G., Deng, W., He, Y., and Ramsis, S. (2006). Hydrochemical characteristics and evolution laws of groundwater in Songnen Plain, Northeast China. *Adv. water Sci.* 17, 20–28. (In Chinese). doi:10.3321/j.issn:1001-6791.2006.01.004

Zhang, L., Liu, Y., Ren, H., and Guo, L. (2016). Application of Stable oxygen and hydrogen isotopes to the verification of Groundwater anomalies. *Seismol. Geol.* 38, 721–731. (In Chinese). doi:10.3969/j.issn.0253-4967.2016.03.017

Zhang, L., Liu, Y., Ren, H., and Ke, Y. (2019). Application of hydrochemistry to the verification of groundwater anomalies. *Earthquke* 39, 29–38. (In Chinese). doi:10.3969/j.issn.1000-3274.2019.01.004

Zhang, L., Liu, Y., Sun, X., and Fang, Z. (2014). A study of water level anomalies using hydrochemical and physical methods. *Seismol. Geol.* 36, 513–522. (In Chinese). doi:10.3969/j.issn.0253-4967.2014.02.019

Zhang, W. (1992). *Observation and prediction of hydrogeochemical earthquake precursors*. Beijing, China: Seismological Pres. (In Chinese).

Zhao, D., Zhou, X., Zhang, Y., He, M., Tian, J., Shen, J., et al. (2023). Hydrogeochemical study of hot springs along the tingri–nyima rift: relationship between fluids and earthquakes. *Water* 15, 1634. doi:10.3390/w15081634

Zhou, R., Zhou, X., Li, Y., He, M., Li, J., Dong, J., et al. (2022). Hydrogeochemical and isotopic characteristics of the hot springs in the litang fault zone, southeast qinghai–tibet plateau. *Water* 14, 1496. doi:10.3390/w14091496

Zhou, Z., Tian, L., Zhao, J., Wang, H., and Liu, J. (2020). Stress-Related pre-seismic water radon concentration variations in the panjin observation well, China (1994–2020). *Front. Earth Sci.* 8, 596283. doi:10.3389/feart.2020.596283

Zhou, Z., Zhong, J., Zhao, J., Yan, R., Tian, L., and Fu, H. (2021). Two mechanisms of earthquake-induced hydrochemical variations in an observation well. *Water* 13, 2385. doi:10.3390/w13172385